International Journal of Applied Engineering Research ISSN 0973-4562 Volume 14, Number 15 (2019) pp. 3381-3395

Application of remote sensing and Geographic Information System (GIS) for the predictability and mapping of Brazzaville's water erosion zones (Congo)

Narcisse Malanda[1*], Guy Dieudonné Moukandi-Nkaya[1], Gilbert Nganga[1], Béthel Aïvan Bagnama Mfoutika[1], Milse William Nzingou Mouhembe[1], Florent Boudzoumou[3], Joseph Mangouende[2]

[1] *École Nationale Supérieure Polytechnique (ENSP),* [2] *École Normale Supérieure (ENS),*
[3]*Faculty of Science and Technology (FST)*

Mechanics, Energy and Engineering Laboratory,
Marien Ngouabi University, BP 69, Brazzaville, Congo.

Summary

The objective of this study is to assess and map areas vulnerable to water erosion in Brazzaville using a qualitative approach, based on the PAP/CAR method and the Geographic Information System (GIS). The data were obtained from Landsat 8 satellite images and processed with ARCGIS software. Of the nine districts of this city, three (Mfilou, Talangai and Djiri) are considered potentially vulnerable to erosion. The latter include watersheds with very steep class slopes (20-35%), and the highest altitudes (440-500). However, the study area is dominated by a tertiary sandy lithology representing about 67% of the total surface area and the friability of materials; loose, non-cohesive soils or Batékés sands. The study also shows that 65% of the study area has low and medium erodibility, and 35% has high and very high erodibility. Descriptive mapping of various forms of erosion shows that gullies, surface gullies and sheet erosion are the most common. The consolidated map of erosion states shows qualitatively the soil losses in the study area, in proportion to the increase in the main factors of water erosion. After combining different maps of the main erosive states, a synthesis was made by producing the consolidated map of these states (integration approach). The latter indicates both potential and current erosion in its different forms: intensities and evolutionary trends. The areas at low and moderate erosion risk correspond to the forms of erosion in medium deep and deep ravines that coincide with the areas at high and very high erosion risk.

Keywords: Remote sensing, Geographic Information System, PAP/CAR model, vulnerability, soil, water erosion, mapping.

1. INTRODUCTION

In recent years, erosion phenomena have become very remarkable in many countries. They are especially frequent in tropical countries where rainfall is a dominant effect. However, with rainfall intensity ranging from about 1054 to 1734 mm/year [1], Congo is not spared from these phenomena and the city of Brazzaville is one of the high-risk areas threatening housing, neighbourhoods, electrical installations, drinking water supply networks, etc. (Figures 1, 2, 3 and 4). But, despite these negative impacts, very few conservatory or even preventive measures are taken to combat soil degradation. The consequences of erosion are such that various disasters and injuries are observed in these localized areas. Thus, we can note the formation of gullies in areas with a remarkable slope and low ground cohesion, the phenomena of silting, landslides, etc. On the other hand, the city of Brazzaville has a strong attraction for citizens, an effect that not only contributes significantly to changing its demographic physiognomy [2], but also accentuates the dynamics of erosion. Similarly, the very strong urban growth of this city (about 79%) is less and less supported by the public authorities, which no longer develop a consistent policy to absorb or anticipate these recurring phenomena, especially in new districts with spontaneous housing. This city is developing uncontrolled urbanization with high anthropogenic activity. It then covers soils composed of a large layer of sandy-sandstone formation [3], [4]. These are powdery and inconsistent soils that reflect their vulnerability to erosion. This phenomenon is also accentuated by the gradual elimination of vegetation cover, especially in slope areas. Then, there is also an uncontrolled occupation of the hills that triggers this generalized phenomenon (erosion) and whose manifestations vary with their geomorphology.

The city is confronted with various problems of soil degradation, which sometimes take the form of real natural disasters. Thus, the result is the destruction of the environment, infrastructure and various works including water and soil pollution [5], [6], [7], [8], [9], [10] et [11]. However, the occupation of high altitude areas, without prior development, increases their sensitivity to water erosion. On the other hand, the occupation of low-lying areas leads to flooding and pollution problems due to poor management of runoff water. Work already undertaken shows that the negative effects of water erosion are significant and sometimes catastrophic on the environment and the economy [5], [9] et [12].

In short, these degradations constitute a major challenge in sustainable development, sanitation and the quality of life of populations. Since the control of water or mass erosion must first and foremost be preventive, it is then necessary to identify and develop a map of the intensity of soil erosion using remote sensing data in an environment (Geographic Information System) by considering the different catchment areas of this city and by taking into account the sensitivity of these soils to erosion. The assessment of the risk of erosion is therefore necessary based on the analysis of many factors involved in the erosive process. Several methods and tools have been developed by researchers for mapping and qualitative estimation of water erosion, including USLE, RUSLE, LEAM, PAP/CAR, etc., including Wischmeier's empirical models that assess soil loss.

In this study, the PAP/RAC (Priority Activities Programme/Regional Activity Centre) approach, which is a qualitative and coherent practical approach, and which has proved to be very useful for mapping and modelling water erosion, was used for this study [13], [12], [14], [15], [16], [6] and [7]. The use of geographic information systems (GIS) and remote sensing has made it possible to process the large amounts of data collected for the study area, to model and spatialize water erosion phenomena [17], [18], [19], [20] and [21]. Thus, this work aims to identify, spatialize and map particularly eroding areas for predictability.

Figure 1 : View of erosions in the Lebled district

Figure 2 : Destruction of a plot in the Makabandilou district

Figure 3: Flooding in district 9 Djiri

Figure 4 : Silting in the arrondissement 7 Mfilou

2. MATERIAL AND METHODS

2.1. Geographical location

The city of Brazzaville lies between latitude coordinates -4°15'56S, and longitude 15°16'59E. The average altitude is about 301 m. It currently has nine (09) districts which are Makélékélé, Bacongo, Poto-Poto, Moungali, Ouenzé, Talangaï, Mfilou, Madibou, Djiri. From a hydrographic point of view, this city is also watered by the Djiri rivers in the north and Djoué in the south. In addition to these tributaries of the Congo River, there are also the Mfilou River in the west and the Tsiémé River in the northern zone. The Mfoa River, which receives water from one of its branches, the Madoukou River, in the central zone, also flows into the Congo River (Figure 5, Figure 6).

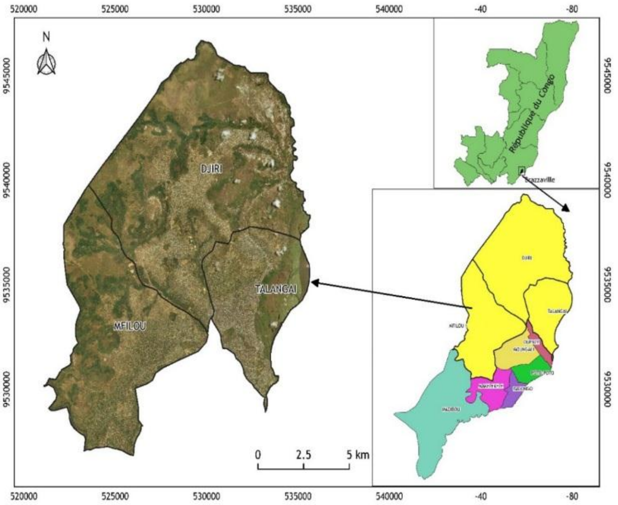

Figure 5: Presentation of the study area

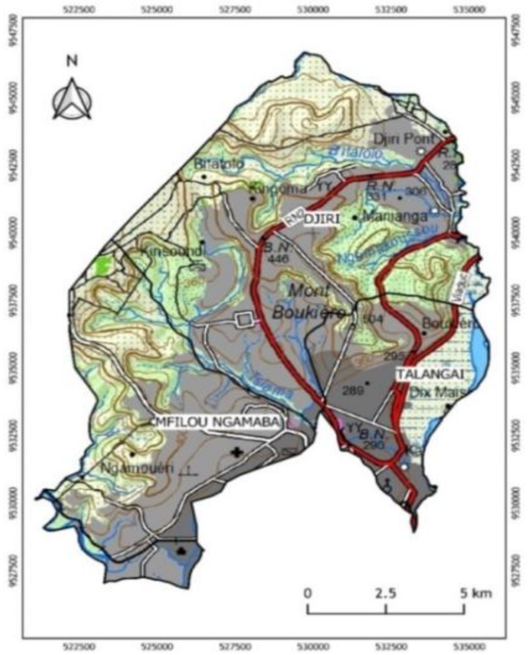

Figure 6: Brazzaville Topographic Background

2.2. Equipment

1- An Extres-type, GPS for tacking geographic;
2- GIS Q GIS software 3.4.2. Madeira, ARGIS 10.4 Software;
3- Satellite images ASTER GLOBAL DEM and Landsat 8 OLI/TIRS C1 Level-1 ;
4- The Digital Terrain Model (DTM) (Figure 7),[22],[20]
5- Data on soil potential and resources (Figure 9), change in vegetation cover (Figure 10)

- **Landsat 8 OLI image**

The image was acquired in 2018 and subsequently generated. The cartographic projection is the UTM (Universal Translate Mercator) of zone 33 and the reference coordinate system is the WGS84. This image was used to develop the vegetation cover map and land use map (Figure 8).

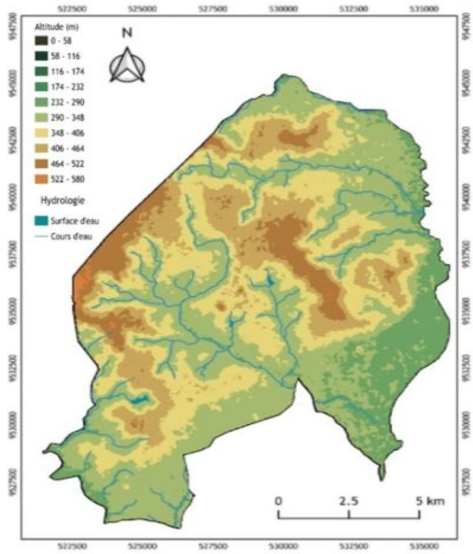

Figure 7: Digital terrain model [22]

Figure 8: Landsat 8 image cut to level [22]

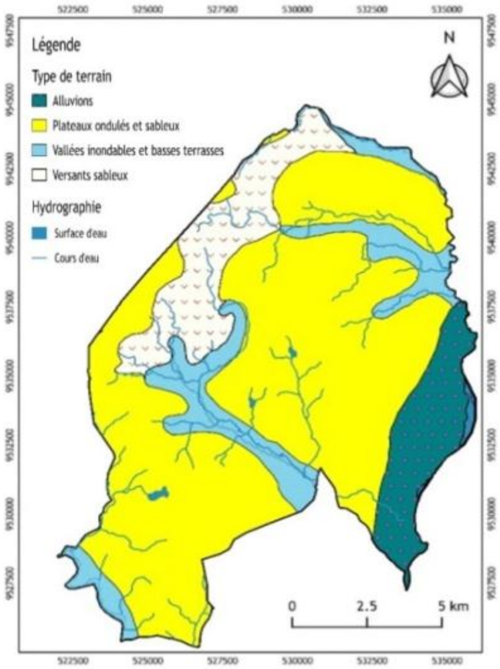

Figure 9: Map of soil potential and resources *(source : Centre de Recherche Géographique et de Production Cartographique (CRGPC)*

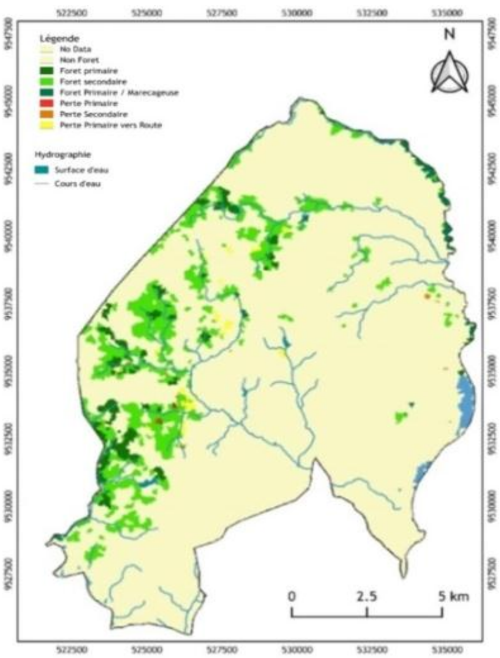

Figure 10: Map of forest cover change

(source : Centre de Recherche Géographique et de Production Cartographique (CRGPC)

✓ **Climate context**

Studies by Samba and Nganga (2011) have shown that long climate data series subdivide Congo into two climate types: equatorial climate in the north and humid tropical climate in the south. The area of the city of Brazzaville belongs to the humid tropical climate. This climate is under the predominant influence of low intertropical pressures from October to May and high subtropical southern pressures from June to September. Cloud cover is all the more important and almost permanent as the activity of the inter-tropical convergence zone (ITCZ) is reversed. It directly influences sunstroke and solar radiation. It is also characterized by an alternation of two seasons: a rainy and warm season that extends from November to April with very heavy rainfall and a dry and cool season from June to September during which the water balance is probably in deficit. October and May provide a transition period for the entry and exit of the dry season [23], [24].

✓ **Geological context**

The geological features of the study area include a clayey to clayey and marly sandstone formation called Stanley Pool in the northeast, in the middle and for the most part a soft sand and sandstone formation, polymorphic sandstones topped by sandy silts called Batékés sands. And more, in the southwest, the so-called Inkissi formation made of feldspar sandstones, arkoses and arkotic conglomerates. Near the river, the sands have been eroded, and replaced by sandy-clayey alluvium of variable thickness that may contain muddy and peaty levels, and covered with swampy areas, etc. In general, these soils are essentially sandy with some particular elements such as sandstone. These are soils with low water retention capacity and therefore have low resistance to rainwater runoff and runoff [10], [3], and [4].

✓ **Geomorphological context**

The relief of Brazzaville is essentially made up of a series of hills, plains and plateaus.

This relief is a transition between the relief of the Batékés plateaus in the north and that of the cataracts plateau in the south.

It thus makes it possible to distinguish three zones:

- The first area is an alluvial plain located to the east and northeast with an altitude between 275 and 285 m. This area is often subject to flooding during the rainy season, flooding due to the absence of slopes and high occupancy. The boroughs not found there are: Talangai, Ouenzé, certain districts of Moungali and Poto-Poto;
- The second area is a plateau with an average altitude of between 300 and 320 m. This zone is made up of the following boroughs: Bacongo, Makélékélé, Mfilou-Ngamaba, and other districts of Poto-Poto and Moungali ;
- The third area is the former alluvial terrace that develops on the right bank of the Djoué (figure 6) [25].

✓ **Contexte phytographique**

The vegetation in the study area consists of only two types of formations, the high closed tree formation, formed by the mesophilic forest and the high open grassy formation, formed by the savannah at Loudetia Demeusei. The Savannah at

Loudetia Demeusei covers the polymorphic Batékés sandstones. These sandstones decompose into sands that determine a relief entirely formed by a succession of rounded hills with steep slopes separated by dry valleys. It is a clear, low, loose grassy mat formation that does not occupy the entire soil surface, allowing many other species to develop.

The shrub stratum is thin, the few shrubs are small.

2.3. Method

✓ **PAP/CAR method**

The water erosion susceptibility map is established using the PAP/CAR method, which essentially consists of three approaches (Figure 11).

The potential erosion assessment model developed by PAP/CAR is the result of three phases, namely:

- The predictive approach;

- The descriptive approach;

- The integration approach

Satellite images were processed at the field scale with appropriate mapping software (QGIS...) [16], [6].

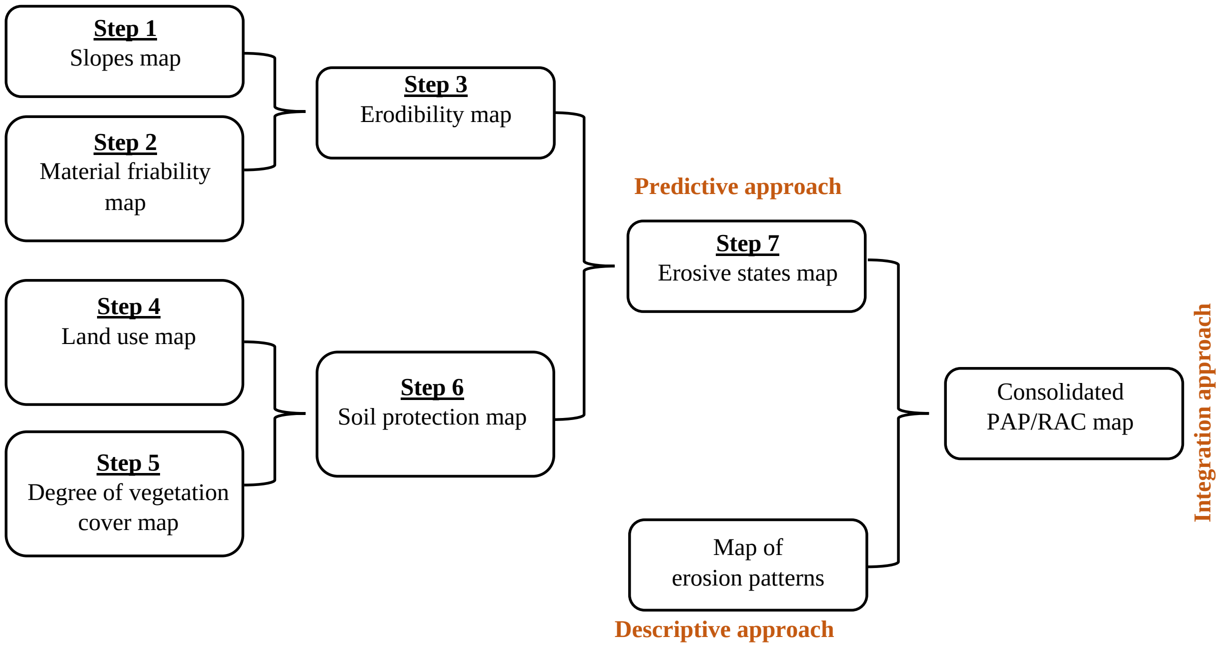

Figure 11: PAP/CAR approach [13], [12], [16] and [6]

Table 2: Classification of predictive approach parameters according to PAP/CAR (1998).

Slope			Lithofacies		
Classes	**Inclination**	**Degree**	**Classes**	**Resistance**	**Type of equipment**
1	None to low	(0-3%)	(a)	Very strong	Unaltered compact rocks, highly cemented conglomerates, etc.
2	Moderate	(3%-12%)	(b)	Strong	Fractured or moderately altered cohesive rocks or soils.
3	Abrupt	(12%-20%)	(c)	Average	Sedimentary rocks or soils that are slightly or moderately compacted (slate, shale, marl, etc.)
4	Very steep	(20%-35%)	(d)	Low	Rocks and/or soils with low resistance or strongly/deeply altered (marl, gypsum, clay slate,
5	Extreme	(>35%)	(e)	Very Low	Soft, non-cohesive sediments or soils and detrital materials.

Land use planning			Degree of vegetation cover		
Classes	**Protection**	**Type of coverage**	**Classes**	**Protection**	**Degree of vegetation cover**
1	Very Low	Dry cultivation (herbaceous)	1	Low	<25%
2	Low	Arboriculture, online cultivation and reforestation	2	Average	25%-50%
3	Average	Intensive culture of proximity to housing	3	Strong	50%-75%
4	Strong	Forests	4	Extreme	>75%
5	Very strong	Dense shrubs			
6	Extreme	Sparse shrubs, pastures			

Table 3: Land use matrix / land cover

Land use planning	Degree of vegetation cover			
	1	**2**	**3**	**4**
1	5(MB)	5(MB)	4(B)	4(B)
2	5(MB)	5(MB)	4(B)	3(M)
3	3(M))	2(A)	1(MA)	1(MA)
4	4(B)	3(M)	2(A)	1(MA)
5	5(MB)	4(B)	3(M)	2(A)
6	5(MB)	4(B)	3(M)	2(A)

With : Very High (MA), High (A), Medium (M), Low (B) and Very Low (MB).

Table 4: Soil protection degree matrix / degree of erodibility.

Degree of soil protection	Degree of erodibility				
	1(EN)	**2(EB**	**3(EM)**	**4(EA)**	**5(EX)**
1(MA)	1	1	1	2	2
2(A)	1	1	2	3	4
3(M)	1	2	3	4	4
4(B)	2	3	3	5	5
5(MB)	2	3	4	5	5

With : Very high degree (1), High degree (2), Significant degree (3), Low degree (4), Very low degree (5).

Table 5: Slope matrix / friability

Slope classes	Class of lithofacies				
	1(a)	**2(b)**	**3(c)**	**4(d)**	**5(e)**
1	1(EN)	1(EN)	1(EN)	1(EN)	2(EB)
2	1(EN)	1(EN)	2(EB)	3(EM)	3(EM)
3	2(EB)	2(EB)	3(EM)	4(EA)	4(EA)
4	3(EM)	3(EM)	4(EA)	5(EX)	5(EX)
5	4(EA)	4(EA)	5(EX)	5(EX)	5(EX)

With : Low (EN), Moderate (EB), Medium (EM), Strong (EA), Extreme (EX).

✓ **The predictive approach (map of erosive states)**

This approach is mainly based on data processing in order to assess the degree of soil protection and the degree of erodibility in several stages:

- The elaboration of the slope map.
- The elaboration of the lithofacies map.
- The erodibility map.
- The land use map.
- The elaboration of the vegetation cover map.
- The soil protection map.
- The map of erosive states.

✓ **The descriptive approach**

This approach gives a real picture of the different forms of erosion existing in the study area and their degrees of exposure to degradation.

✓ **The integration approach**

It is the superposition of the map of erosive states obtained by thematic mapping and the map of erosion forms obtained by direct descriptive mapping of erosion forms in the field or by satellite images. The mapping system used and corresponding to the PAP/CAR is a digital method based on descriptive data of the selected sites (topography, land use, lithology) and spatial data from the Geographic Information System (GIS) assimilated to thematic maps; in particular Landsat 8 and Google Earth satellite images, field observations, digital terrain model (DTM) from ASTER satellite images.

The coordinate system used is WGS84/UTM Zone 33S or EPSG32733, [22].

3. RESULTS AND DISCUSSION

3.1. Interpretation of the results

✓ **Predictive approach**

All results mentioning erosive states according to the PAP/CAR approach are presented in the following maps:

✓ **Contour maps**

These maps allow us to situate ourselves on the different altitudes of the study area. It also makes it possible to highlight the different watersheds. The Digital Terrain Model (DTM) and contour lines show that the altitudes at the study area range from 20 to 500 metres. Altitudes from 320 m and above are almost considered to predominate in the study area because they are found in the north, east and southeast (Figures 12 and 13).

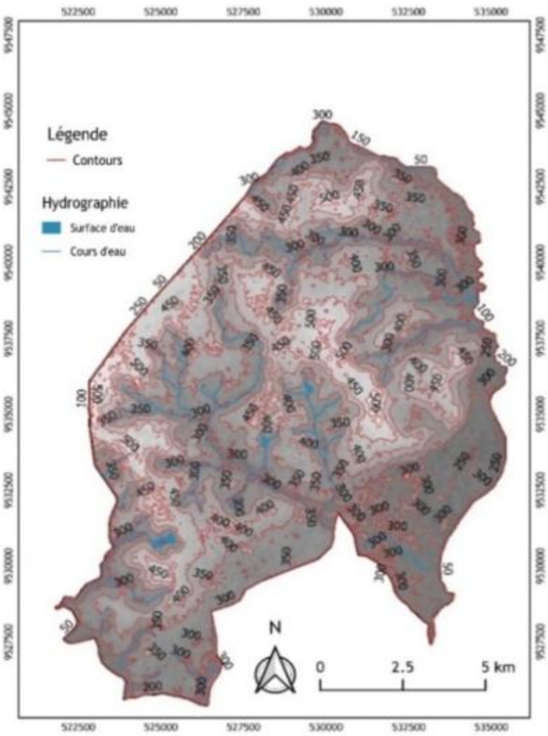

Figure 12: Level curves

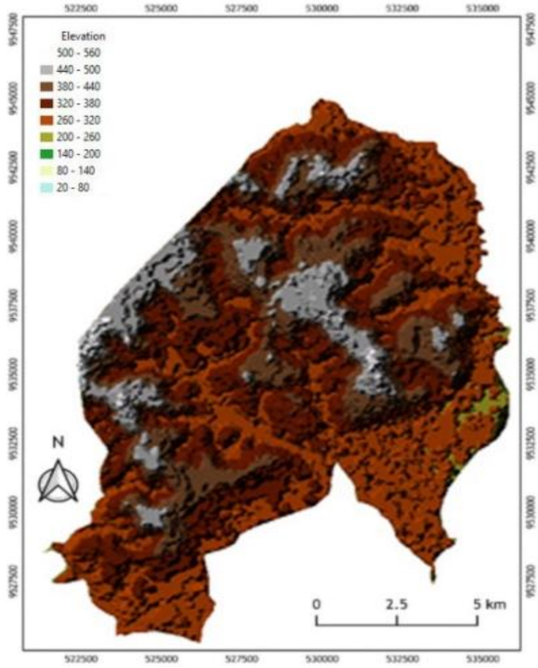

Figure 13: Map defining altitudes

✓ **Slopes map**

Slope is a major factor in assessing the sensitivity of land to erosion.

The slopes vary between 0 and 35%. The more the slope map shows that the degree of slope is generally steep (12-20%) throughout the study area.

This class predominates as it is found throughout the area. The moderate class (3-12%) also occupies a large part of the area of this zone and mixes with the moderate class.

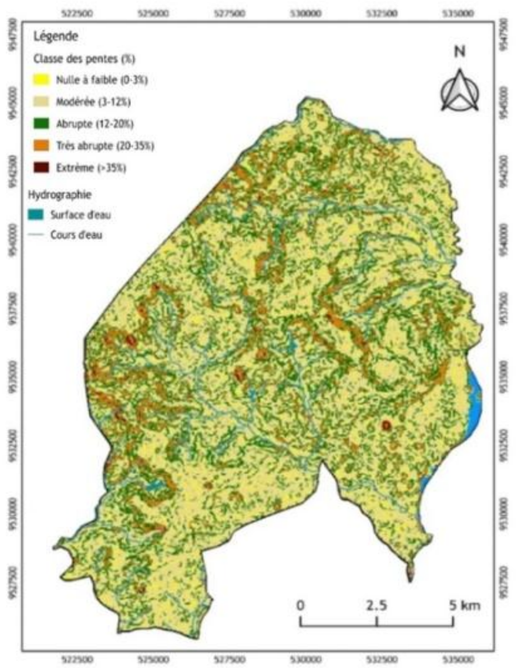

Figure 14: Slopes map

We can also notice the very steep class (20-35%) at the highest altitudes appear as ligaments on steep slopes.

The zero class with a low percentage (0-3%) is distinguished by only a few tasks. And finally, the extreme class (>35%) represents only a few features above the very steep class.

Thus, this map shows that these slopes make the study area, particularly districts 7 and 9 (Mfilou and Djiri), sensitive to the erosive action of rainfall and the higher activity of runoff water, thus causing considerable gullying (Figure 14).

✓ **Map of the Lithofacies**

The Lithofacies Map shows that the study area is dominated by a tertiary sandy lithology which represents 67% of the total surface area, followed by Stanley Pool Secondary sandstone (27%), distributed to the east and along the Congo River, and then just south, at the Djoué River, we find Inkissi sandstone which represents only 6% of the study area (Figure 15).

The Batékés sands are very dominant [4].

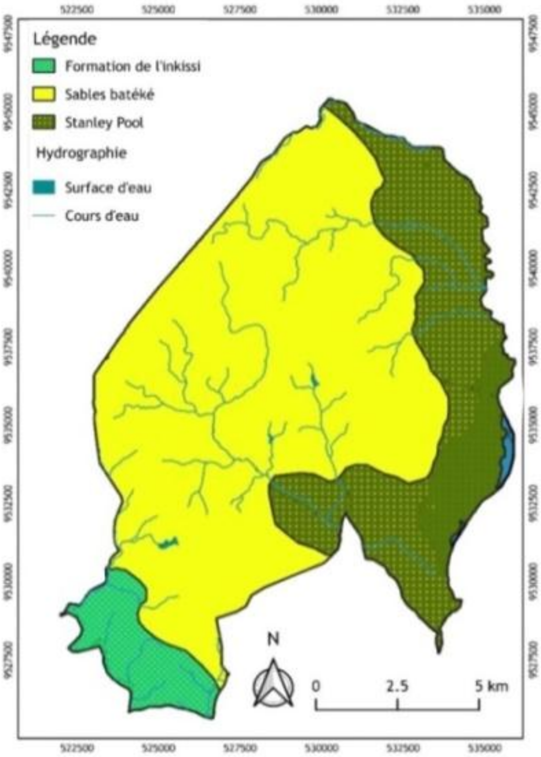

Figure 15: Map of lithofacies

✓ **Material friability map**

Based on the vulnerability of substrates to erodibility, the different types of materials exposed on the geological map have been divided into 5 friability classes (material resistance to erosion).

Thus, the class (e) formed by loose, non-cohesive sediments or soils and detrital materials (Batékés sands) occupies most of the area with 67% (113 km²) of surface area.

It is the lowest class and therefore highly sensitive to erosion.

Then comes the weak class (d) formed by rocks and/or soils that are not very resistant or strongly/ deeply altered, which represents 27% of the total surface area, or 46 km2 (Figure 16).

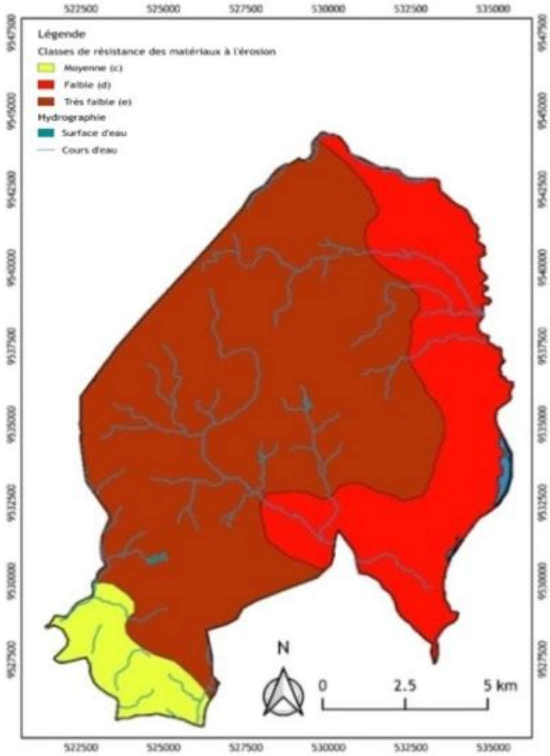

Figure 16: Material resistance map

The middle class of erosion sensitivity (c), corresponding to slightly or moderately compacted sedimentary rocks or soils (Inkissi sandstone) occupies only 6% of the study area (11 km²).

The low sensitivity to erosion class (a) and the high sensitivity class (b) are not mentioned in the study area because of the different geological layers involved.

✓ **Erodibility map**

The erodibility map is the result of the superposition of the slope map and the erosion resistance map of materials (Table 1).

Table 1: Resulting Erodibility Matrix

Slope	Resistance class	Erodibility
1 (3)	a	[EN (9) ; EN (30) ; EB (70)]
2 (12)	b	[EB (18) ; EM (39) ; EM (79)]
3 (20)	c (6)	[EM (26) ; EA (47) ; EA (87)]
4 (35)	d (27)	[EA (41) ; EX (62) ; EX (102)]
5 (59)	e (67)	[EX (65) ; EX (86) ; EX (126)]

The polygons resulting from the cross product of the two tables are classified according to a matrix to prioritize the terrain according to the degree of erodibility.

Erodibility is always extreme when the slope is steep and/or the terrain is of low resistance.

The spatial distribution of the different erodibility classes shows that over the entire formation of the Batékés sands, erodibility is moderate (EM) and that on very steep slopes, erodibility formation is extreme (EX). This is due to its friability (Figure 17), (Table 1).

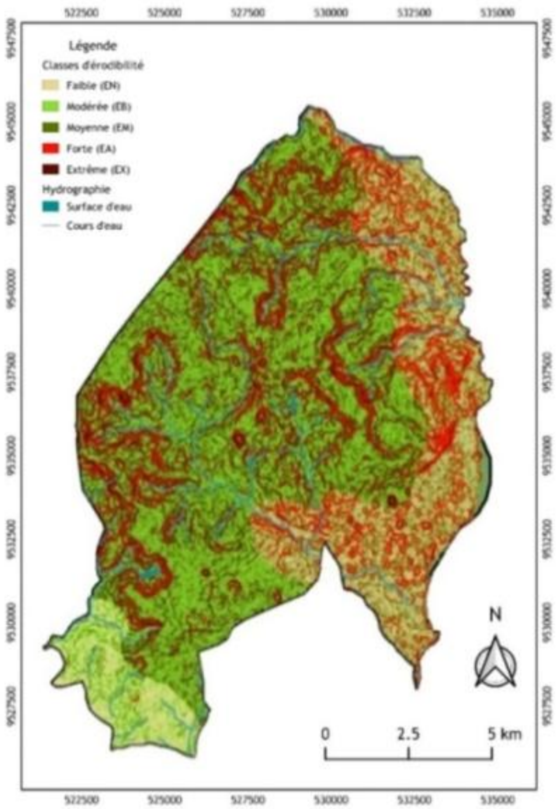

Figure 17: Erodibility map

The values of the degree of erodibility are: EN(9 ;30); EB(18; 70) ; EM(26 ;39 ;79) ; EA(41 ;47 ;87) ; EX(62 ;65 ;86;102;126). On the Stanley Pool formation, there are three types of erodibility: the weak (EN) which focuses on the whole formation, the strong (EA) which appears very visibly and the average (EM) which is mixed with the others.

At the sandstone level of the Inkissi, which is the most resistant formation in the area, there is a high proportion of low (EN) and moderate (EB) erodibility.

✓ **Land use map**

Land use is dominated by the bare land class, which occupies almost the entire study area.

It covers more than 60% of the total area of the study area. It is generally found on lands with a moderate and steep slope. It is scattered throughout the study area, mainly in the centre and on the hillsides.

It is the area of land on which there is no vegetation cover. The grassy savannah class is the second most important class (Figure 18).

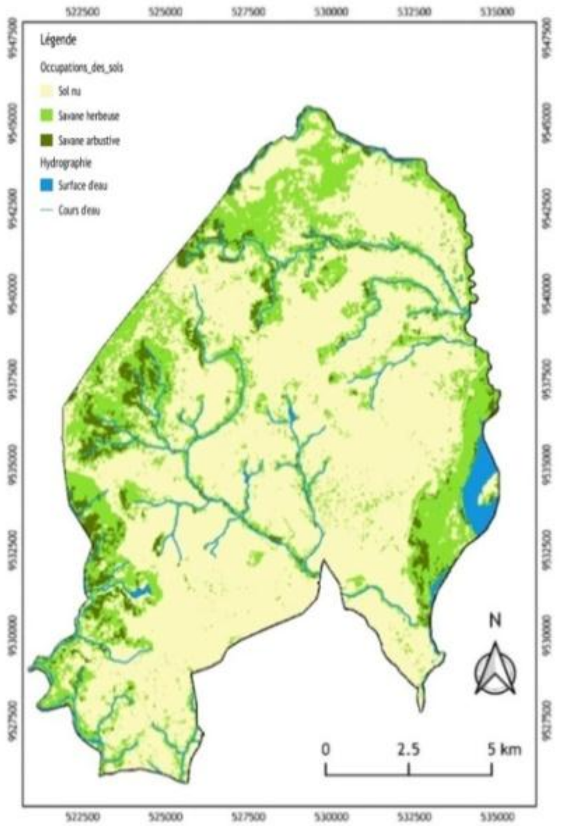

Figure 18: Land use map

It is mainly located on the outskirts of the study area. Next comes the shrubby savannah, which represents the densest vegetation in the study area.

These are the only types of vegetation cover found in the area.

Thus, the predominance of bare soils (land without vegetation cover) over almost the entire study area makes the soils even more vulnerable to erosion.

✓ **Vegetation cover map**

The vegetation cover depends on the growth and development of vegetation in relation to the variation in climate erosion. The

NDVI (Normalized Difference Vegetation Index) vegetation index for the study area was calculated from the Landsat 8 satellite image taken in 2018. It shows four classes of NDVI values. The highest values (0.349; 0.441) correspond to the shrubby savannah areas where vegetation is most dense in the study area. High values (0.278; 0.349) represent dense vegetation, medium density vegetation is represented by values between (0.207; 0.278) and low values (0.207; 0.068) correspond to sparse vegetation areas and croplands.

The three districts of Mfilou, Talagai and Djiri are characterized by very dense vegetation of the density class (>75%) with often degraded or absent shrub cover. The density class (50%-75%) (dense vegetation) is also lower than the first one. It surrounds the very dense vegetation in the study area, while the average vegetation class (25%-50%) represents the most distributed part of the vegetation in the study area (Figure 19).

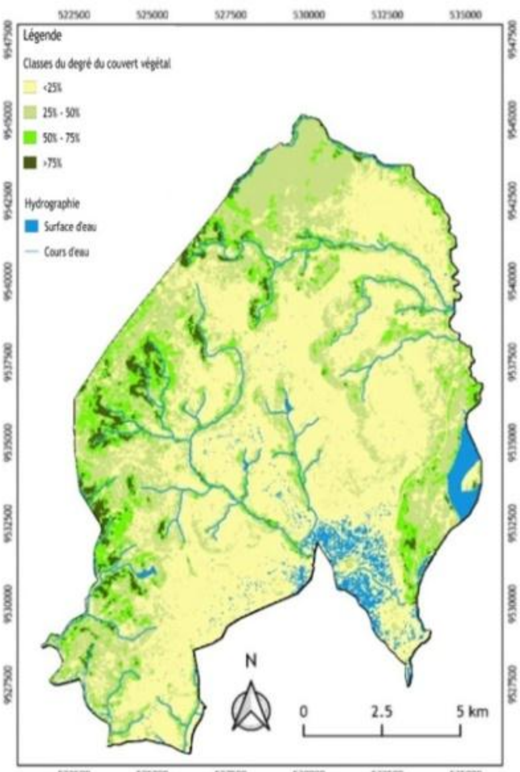

Figure 19: Vegetation cover map

✓ **Soil protection map**

Vegetation protects soils from ablation by reducing the energy of erosive agents by reducing the energy of rain erosion by intercepting raindrops through the upper parts of the plants.

The values of the degree of soil protection are: MB(3,067 ; 3,208 ; 4,067 ; 4,208 ; 4,208 ; B (3,278 ; 4,278 ; 4,349) M(2,067 ; 3,349) ; A(2,208) ; MA (2,278 ; 2,349).

The soil protection map showed different areas divided into five classes: very low (MB), low (B), medium (M), high (A) and very high (MA).

The very low protection (MB) class is found throughout the study area, in the areas that contain a Batékés sands lithofacies and dwellings. In fact, the entire study area is not protected.

The low protection class (B) surrounds almost all the areas of the high (A) and medium (M) class which extends along the watercourses.

The very high class (MA) is almost identical to the high class (A).

All other classes are in uninhabited or sparsely populated areas. High and high erosion areas correspond to areas of high human activity where relatively large human populations live.

The poor protection of the study area is explained by a very degraded vegetation cover due to the high need for cropland and overgrazing (Table 2), (Figure 20).

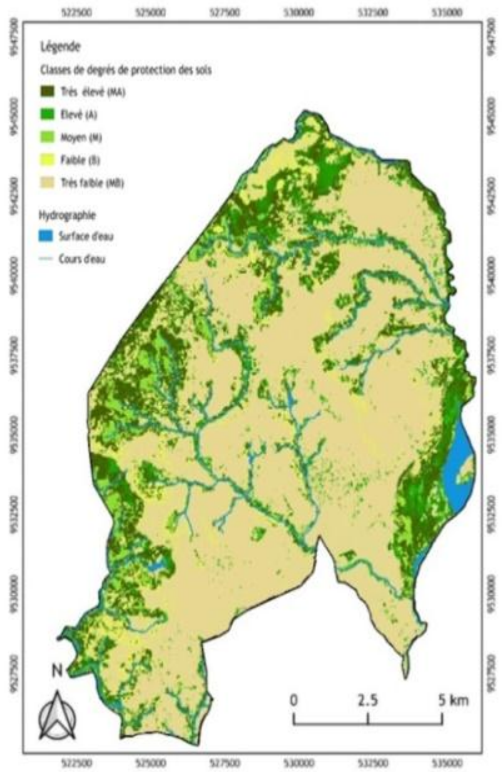

Figure 20: Soil protection map

Table 2: Resulting matrix of the soil protection map

Occupation du sol	Degré du couvert végétal	Protection des sols
1 (2)	1 (0,0667)	[MB (4,067) ; MB (4,208) ; B (4,278) ; B (4,349)]
2 (3)	2 (0,208)	[MB (3,067) ; MB (3,208) ; B (3,278) ; M (3,349)]
3 (4)	3 (0,278)	[M (2,067) ; A (2,208) ; MA (2,278) ; MA (2,349)]
	4 (0,349)	

✓ **Erosive states map**

The map of erosive states shows five classes representative of the degrees of erosion.

These are the very low, low, notable, high and very high classes.

The distribution of areas on the map of erosive states shows that the classes at very low risk of erosion are spread out at the bottom of the Inkissi formation and is surmounted by the notable class and some trace of high degree.

The sandy formation of the Batékés is classified as a risk level.

The Stanley Pool on the other hand is made up of a mixture of the lower class and the degree at risk.

We can see by this map, the influence of the resistances of the materials and therefore of the lithological formations and slopes on the vegetation cover of the area (Figure 21), (Table 3).

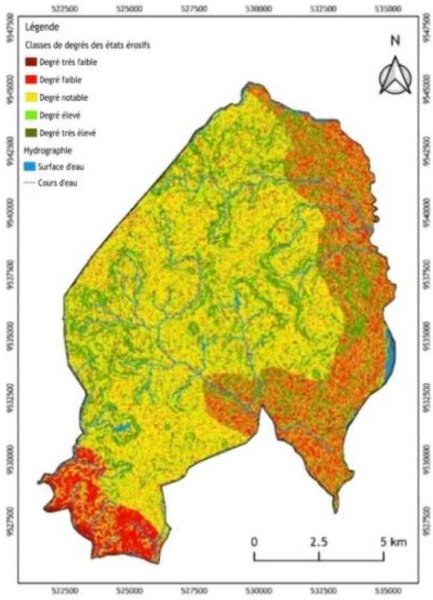

Figure 21: Erosive states map

Table 3: Erosive state polygon matrix

Degree of soil protection	**Degree of erodibility**	**Erosive state**
MA (2,278 ; 2,349)	EN (9 ; 30)	[1] [11,28 ; 32,28 ; 11,35 ; 32,35] ; [1] [72,28 ; 72,35 ; 20,28 ; 20,35] ; [1] [81,28 ; 28,28 ; 41,28 ; 81,35 ;28,35 ;41,35 ;] ; [2] [89,28 ;43,28 ;49,28 ;89,35 ;43,35 ;28,35 ;49,35] ; [2][67,28 ;88,28 ;128,28 ;64,28 ;104,28 ;67,35 ;88,35 ;128,35 ;64,35 ;104,35]
A (2,208)	EB (18 ; 70)	[1] [11,21 ;32,21] ; [1] [72,21 ;20,21] ; [2] [81,21 ;28,21 ;41,21] ; [3] [89,21 ;43,21 ;49,21] ; [4] [67,21 ;88,21 ;128,21 ;64,21 ;104,21]
M(2,067 ; 3,349)	EM (26 ; 39 ; 79)	[1] [11,07 ;32,07 ;12,35 ;33,35] ; [2] [72,07 ;73,35 ;20,07 ;21,35] ; [3] [81,07 ;82,35 ;28,07 ; 29,35 ;41,07 ;42,35] ; [4] [89,07 ;90,35 ;43,07 ;44,35 ;49,07 ;50,35] ; [4] [67,07 ; 68,35 ;88,07 ;89,35 ;128,07 ;129,35 ;64,07 ;65,35 ;104,07 ;105,35]
B(3,278 ; 4,278 ; 4,349)	EA(41 ; 47 ; 87)	[2] [12,28 ;13,35 ;33,28 ;34,35] ; [3] [73,28 ;74,35 ;21,28 ;22,35] ; [5][82,28 ;83,35 ;29,28 ;30,35 ;42,28 ;43,35] ;[90,28 ;91,35 ;44,28 ;45,35 ;50,28 ;51,35] ; [5][68,28 ;69,35 ;89,28 ;90,35 ;129,28 ;130,35 ;65,28 ;66,35 ;105,28 ;106,35]
MB(3,067 ; 3,208 ; 4, 067 ; 4,208)	EX(62 ; 65 ; 86 ; 102 ; 126)	[2][12,21 ;33,21 ;12,07 ;33,07 ;13,21 ;34,21 ;13,07 ;34,07] ; [3][73,21 ;21,21 ;73,07 ;21,07 ;74,21 ;22,21 ;74,07 ;22,07] ; [4][82,21 ;29,21 ;42,21 ;82,07 ;29,07 ;42,07 ;83,21 ;30,21 ;43,21 ;83,07 ;30,07 ;43,07] ; [5][90,21 ;44,21 ;50,21 ;90,07 ;44,07 ;50,07 ;91,21 ;45,21 ;51,21 ;91,07 ;45,07 ;51,07] ; [5][68,21 ;89,21 ;129,21 ;65,21 ;105,21 ;68,07 ;89,07 ;129,07 ;65,07 ;105,07 ;69,21 ;90,21 ;130,21 ;66,21 ;106,21 ;69,07 ;90,07 ;130,07 ;66,07 ;106,07]

3.2. Descriptive approach to erosion forms

The distribution of erosion patterns in the study area shows that the deep (C4) and moderately deep (C3) ravines as a whole do not represent a large portion of the study area's surface area.

They are most often found on sloping ground or on slopes.

Rather, surface gullies and gullies (D2) and sheet erosion (L23) are the most common.

The presence of these two forms of erosion, especially near rivers and water surfaces, can be explained by the vulnerability of the land, the action of rivers and by anthropogenic actions (Figure 22).

3.3. Integration approach: creation of the consolidated erosion map

The superposition of the erosion status map and the erosion pattern map has provided a mapping product that reflects the reality of the state of soil degradation and the trend of future erosion trends.

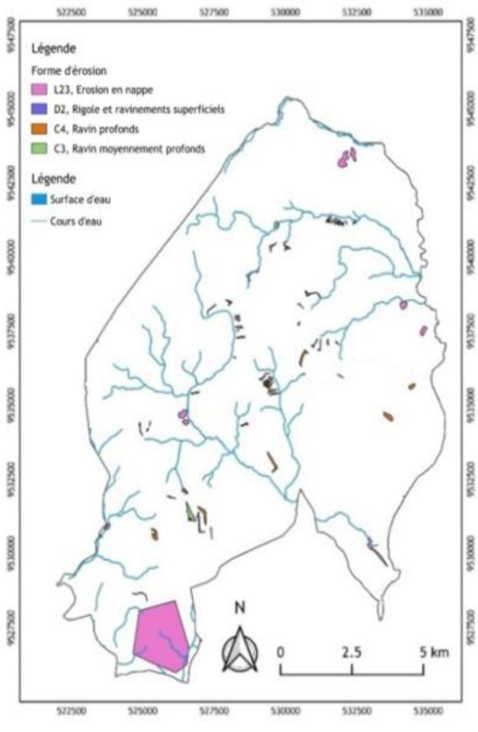

Figure 22: Map of erosion patterns

It resulted in the final cartographic product identifying and evaluating both potential (predictive) and current erosion in its different forms, intensities and evolutionary trends.

The areas at low and moderate risk of erosion correspond to the types of erosion such as gullies and surface gullies and sheet erosion. While the forms of erosion in medium deep, deep ravines coincide with areas at high and very high risk of erosion (Figure 23).

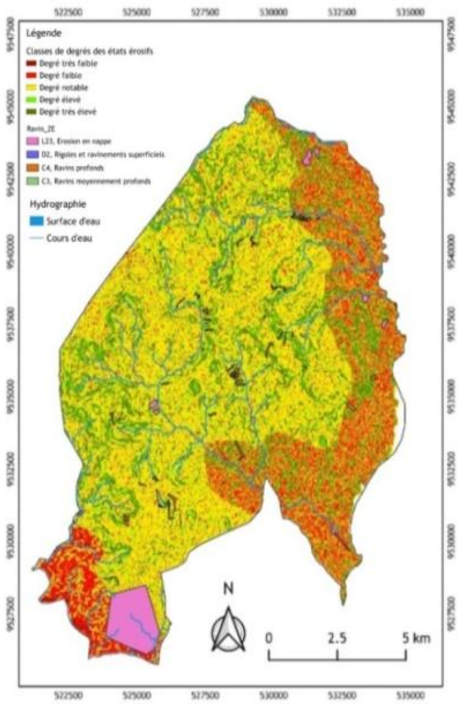

Figure 23: Consolidated map of erosive states

DISCUSSION

The results discussed concern the effects generated by water erosion based on soil classification parameters and geomorphology.

Several studies have been carried out using different approaches, including prediction and predictability of water erosion risks, modelling and mapping of soil sensitivity to erosion.

These studies, which often have different methodological approaches, mostly show the predominance of sheet erosion in the different catchment areas, followed by erosion in gullies and gullies, superficial, in medium deep ravines [6], [26], [27], [8], [12], [28], [29], [30], [31] and [32].

Compared to the USLE, RUSLE and other approaches based on the general soil loss equation, the PAP/CAR method is more qualitative.

Thus, the entire erosive process highlighted, taking into account the maps of slopes, altitudes, lithology, vegetation cover... leads to the elaboration of the final map of erosive states which translates the data from the analysis of the spatial distribution of the factors taken into account in the model and, then, the erosive process. Thus, the analysis of this consolidated map (Figure 23) shows several degrees of erosive states (very low, low, notable, high and very high).

This mapping is consistent with the maps of the physical parameters mentioned in the study area [27], [6] and [31]. Similarly, in relation to the slope map, the (steep) class for the slopes that are predominant in the study area suggests an acceleration of water runoff leading ipso facto to gullies. It can thus be noted that erosion rates increase, significantly with slope, and the dominance of undeveloped soils thus showing remarkable erodibility; this contributes to considerably increasing soil losses.

In general, it can be said that the areas most threatened by the risk of erosion are mainly located in hill areas [6], [12], [8].In general, the results obtained through the various maps also show that the soils covering the study area and specifically the Mfilou, Talangai and Djiri districts are ultimately affected by several factors favouring erosion. These include the importance of slopes, low vegetation cover, material reliability and soil erodibility. The loss of vegetation cover destroys soil protection from ablation by reducing the energy of erosive agents by reducing the energy of rainwater erosion by intercepting raindrops with plants [12]. Some of the results obtained in this study are comparable to those of Koussa and Bouziane (2018), Ben Rhouna, 2018 and Setywan et al (2017). Indeed, these phenomena occurred in watersheds with a remarkable slope, a known material friability and a relatively low vegetation cover.

CONCLUSION

Comparison of the results obtained with those of the previous studies listed above shows that taking into account the temporal variability of the erosion process, the geomorphology of different basins and even rainfall has an impact on the intensity of erosion. Based on this observation, it can be seen that the risk of erosion over time is much higher in mountainous areas with almost no vegetation cover. Thus, in the light of the results obtained and at this stage of our research, the prevention of these disasters lies in monitoring the temporal variation of the erosive process, pending the implementation of a real policy of land development and remediation. In all cases, this is a phenomenon to be reduced. In the end, despite the differences that can sometimes be significant in terms of methodological approach, study area data, climate and other parameters, the results obtained are very similar to some of the work already undertaken.

This study can be further developed on some aspects such as the quantification of soil loss or with other data collection tools. This study allowed us to model from multi-source data the areas and GIS sensitive to water erosion from maps using the PAP/CAR approach. The forms of water erosion prevailing in the area are sheet erosion due to the beating of rains on open surfaces (house courtyards, terraced areas still unexploited, gully erosion due to the energy of runoff along slopes or slopes, and mass erosion due to gravity on the slope. These three forms of erosion lead to significant soil loss and mass degradation. The qualitative study of potential erosion, based on natural factors (slope, lithology, vegetation cover and land use, etc.), made it possible to analyse and understand the problems of the study area in terms of erosion risk. It then made it possible to make a general diagnosis of the potential risk of water erosion specifically in the districts (Mfilou, Talangaï and Djiri) which are characteristic of catchment areas with steep slopes.

Thus, this work is intended to be the creation of a multi-source database on the study area, with the contribution of the Geographic Information System (GIS) and remote sensing. The predictive phase provided information on the current state of land degradation based on the degree of influence of the various factors that control water erosion. It shows that about 65% of the area studied has a low and medium erodibility and 35% a high and very high erodibility. The descriptive approach has shown that soil degradation and loss are manifested by different forms of water erosion with gullies and surface gullies and groundwater erosion predominating. The superposition of the predictive and descriptive phases highlighted the global trends in soil surface evolution.

Also, some very degraded states coincide with spectacular forms of erosion and others more stable with minor forms of erosion or even stable areas. More sensitive areas require continuous, preventive and priority action.

ACKNOWLEDGEMENTS

The authors would like to thank the Director and staff of the Centre de Recherches Géographiques et de Production Cartographique (CRGPC) for their technical assistance..

REFERENCES

[1] Agence Nationale de l’Aviation Civile (ANAC), 2015. Données pluviométriques dans la zone de Brazzaville, 2015

[2] F. Anglade (1985). Migration intérieures au Congo et croissance urbaine de Brazzaville. Disponible en ligne sur http://horizon.documentation.ird.fr/exl-doc/pleins-textes

[3] A. Le Maréchal (1996). Contribution à l’étude des plateaux Batékés – Service géologique. Office de la Recherche scientifique et Technique d’Outre-Mer. [Disponible]. En ligne sur http://horizon.documentation.ird.fr/exl-doc/pleins-textes.

[4] Dominique Schwartz (1986). Les sols des environs de Brazzaville et leur utilisation. ORSTOM. [Disponible] En ligne sur http://horizon.documentations.ird.fr/exl-doc/pleins-textes.

[5] A. Kempena (1), D. Bilembi, F. Boudzoumou and D. Nganga (2014). Methodology for erosion risk zoning in the city of Brazzaville study of case in the urban area. ARPN Journal of earth sciences. ISSN 2305-493X, 2014

[6] A. Ben Rhouma, T. Hermassi and K. Bouajila (2018) Water erosion modelling using the PAP/CAR qualitative method: case of the Sbaihia catchment, Zaghouan. Journal of new sciences. E-ISSN 2286-5314, 2018.

[7] C. Setywan, C. Y. Lee, M. Prawitasari (2017). Application of GIS software for erosion control in the watershed scale. International Journal of scientific and technology research, volume 6, ISSN 2277-8616.

[8] M. Koussa et T. Bouziane (2018) : Apport du SIG a la cartographie des zones à risque d’érosion hydrique dans la région de Djelfa, Algérie. Lebanese Science Journal, Vol. 19, No. 1, 2018.

[9] Kempena (2), F. Boudzoumou, D. Nganga and H. Ray (2014). Cartography of environmental vulnerability to soil erosion of the urban area of Brazzaville using geographic information system (GIS). International Research Journal of Environment sciences, ISSN 2319-1414,

[10] B. Denis et G. De Champs (1970). Les sols de la région de Brazzaville. Office de la recherche scientifique et technique d'outre-mer. [Disponible] En ligne sur http://core.ac.uk/download

[11] Ab. Latif Ibrahim, Siti Yasmin Yaakub, Nor Liyama Mohammad, Tam Tze Huey (2012). Application of Geographic Information System in soil erosion predication. [Disponible]. En ligne sur https://www.researchgate.net/publication/26231780.

[12] H. Ousmana, A. El Hmaidi, Ali Essahlaoui, Hachem Bekri & Abdelhadi El Ouali (2017) : Modélisation et cartographie du risque de l'érosion hydrique par l'application des SIG et des directives PAP/CAR. Cas du bassin versant de l'Oued Zgane (Moyen Atlas tabulaire, Maroc). Bulletin de l'Institut scientifique, Rabat, section Sciences de la Terre (39) : p103-119.

[13] PAP/CAR (1998). Directives pour la cartographie et la mesure des processus d'érosion hydrique dans les zones côtières méditerranéennes. PAP-S/PP/GL.1.split, centre d'activités régionales pour le programme d'actions prioritaires (PAM/PNUE), en collaboration avec la FAO.

[14] S. Boukrim, A. Lahrach, A. Midaoui, F. Benjelloun, M. Benabdelhadi, H. Lahrach, A. Chaouni (2016) : Cartographie de l'érosion qualitative des sols du bassin versant de l'Aoudour (Rif-Maroc). European Scientific Journal (April 2016), vol.12, No.11 ISSN: 1857 – 7881 (Print) e - ISSN 1857- 7431.

[15] Mesrar H., J. Sadiki A., Navas A., Quijano L., Chaouaah (2015). Modélisation de l'érosion hydrique et des facteurs causaux : cas de l'Oued Sahla, Rif Central, Maroc. Zeitschrift für geomorphologie (59) : 495-514. DOI : 10.1127/zfg/20/0169.

[16] J. Tahouri J., L. Karrat, H. Mesrar (2016). Utilisation du modèle PAP/CAR et des outils SIG pour la cartographie et l'évaluation des processus d'érosion hydrique en milieu méditerranéen : cas du bassin versant de l'Oued Asfalou (Maroc). [Disponible] En ligne sur https://www.researchgate.net/publication.

[17] Boggs G., Devonport C., Evans R. et al (2001). GIS-based rapid assessment of erosion risk in a small catchment in the wet/dry tropics of Australia. Land degradation and development, 12, 5, 417-434.

[18] Bachaoui M., Bachoni B., Lhissou R. et al (2014). Modeling and mapping water erosion risk in the high Atlas of Marocco : the Atlas of Beni Mellal as a case in point. Journal of remote sensing and GIS, (2) (1), ISSN: 2052-5583, 40-47.

[19] Akalai N., Hlila R., El Imrani M. et al (2014). Risk of water erosion in coastal watersheds north of Tetuan (Internal Rif, Northen Morocco): Evidences from GIS-based spatial approach. International Journal of innovation and applied studies, 8, 4, 1735-1751.

[20] Serge Riazanoff (1989). Extraction et analyse automatique des réseaux à partir des modèles numériques de terrain. Contribution à l'analyse d'image de télédétection. Thèse de Doctorat, terre, océan et espace, Paris 7 [Disponible]. En ligne sur www.these.fr>1989PA077220.

[21] Adam Kertesz (1993). Application of GIS methods in soil erosion modelling. Comput.environ.and urban systems, vol. 17, pp 233-238. https://doi.org/10.1016/0198-9715 (93) 90018-z.sciences direct

[22] [USGS, 2018]. Science for a changing world [Disponible] En ligne sur https://www.usgs.gov/.

[23] Samba G. and Nganga D. (2011). Rainfall variability in Congo-Brazzaville. 1932-2007. Int. J. Climatol. Published online in wiley.

[24] IPCC, (2007): IPCC Fourth assessment report: climate change 2007 (AR4), IPCC, Geneva, Switzerland.

[25] Codou A. Géographie : La République Populaire du Congo. Collection André-Hatier : 1976, 79 pages.

[26] N. Benzer (2010). Using the geographical information system and remote sensing techniques for soil erosion assessment. Journal of Environment. Stud. Vol. 19. N°5 (2010), 881-886.

[27] L. Khali Issa, K. Ben Hamman-Hab, A. Raissouni, A. El Arrim (2016). Cartographie quantitative du risque d'érosion des sols par approche SIG/USLE au niveau du Bassin versant Kalaya (Maroc Nord Occidental). J. Mater. Environ. Sci 7(8)(2016), ISSN : 2028-2508.

[28] M. Koussa et T. Bouziane (2018) [1]. Apport du SIG à la cartographie des zones à risque d'érosion hydrique dans la région de Djelfa, Algérie, Lebanesse Science Journal, vol. 19, N° 1, 2018.

[29] M. Koussa1 et M. Bouziane (2018) [2] : Apport de SIG a la cartographie des zones à risque d'érosion hydrique dans le bassin versant de Beni Haroun, Mila, Algérie. Geo-Eco-Trop., 2018, 42, 1 : 43-56.

[30] Mushtak T. J. (2003). Application of GIS to estimate soil erosion using RUSLE. Geospatial information Science (quarterly). [Disponible] En ligne sur https://www.academia.cdu.../Application-of-GIS-to-estimate-soil

[31] W. G. Sombroek and J. Antoine (2009). The use of Geographic Information Systems (GIS) in Land resources appraisal. [Disponible] En ligne sur http://horizon.documentation.ird...

[32] A. El Garouani, H. Chen, L. Lewis, A. Tribak et M. Abahrour (2008). Cartographie de l'utilisation du sol et de l'érosion nette à partir d'images satellitaires et du SIG Idrissi au Nord Est du Maroc. [Disponible]. En ligne sur https://hal.archives-ouvertes.fr/hal-00434258.

[33] Sadiki, S. Bouhlassa, J. Auajjar, A. Faleh & J. Macaire (1999) : Utilisation d'un SIG pour l'évaluation et la

cartographie des risques d'érosion par l'Equation universelle des pertes en sol dans le Rif oriental (Maroc) : cas du bassin versant de l'oued Boussouab. Bulletin de l'Institut Scientifique, Rabat, section Sciences de la Terre, 2004, n°26, p. 69-79.